Development of bio-inspired chelates with hydrogen bond donors: synthesis and structure of monomeric metal acetate complexes with intramolecular hydrogen bonds†

Matthew K. Zart,[a] Thomas N. Sorrell,[b] Douglas Powell[a] and A. S. Borovik *[a]

[a] Department of Chemistry, University of Kansas, Lawrence, KS 66045, USA
[b] Department of Chemistry, The University of North Carolina, Chapel Hill, NC 27599, USA

The synthesis of the new multidentate tripodal compounds bis[(N'-tert-butylureido)-N-ethyl]-2-pyridylmethylamine ($H_4$1) and bis[(N'-tert-butylureido)-N-ethyl]-N-methylamine ($H_4$2) is described. These ligands contain two urea-ethylene arms that when deprotonated and bound to a metal ion, position two hydrogen bond donors near the metal center so that formation of intramolecular H-bonds with other coordinated species is possible. The complexes $K[M^{II}(H_2 1)(\eta^1\text{-OAc})]$ and $K[M^{II}(H_2 2)(\eta^2\text{-OAc})]$ (M^{II} = Co and Fe) have been isolated and characterized. The multidentate ligands mediate the mode of acetate coordination: the $[M^{II}(H_2 1)(\eta^1\text{-OAc})]^-$ complexes have a monodentate coordination, whereas in $[M^{II}(H_2 2)(\eta^2\text{-OAc})]^-$ the acetate binds in a bidentate manner. X-Ray diffraction studies reveal that all complexes have trigonal bipyramidal coordination geometries with one of the acetate oxygen atoms being nearly *trans* to the amine nitrogen donor. All the complexes have relatively long M–O bond lengths in comparison with other M^{II}–OAc complexes characterized previously. The complexes exhibit intramolecular H-bonds from the urea NH groups to one of the coordinated oxygen atoms of the acetate, causing a lengthening of the M^{II}–OAc bond distances. The NH · · · O bond lengths and vibrational energies in these acetate complexes support weaker H-bonds than the H-bonding interactions in similar ligand complexes with hydroxo ligands.

Introduction

Hydrogen bonds (H-bonds) in the active sites of metalloproteins are instrumental in regulating activity. Of particular importance are H-bonds that form between amino acid residues and ligands coordinated to active site metal ions. Numerous structural,[1] spectroscopic,[2] and theoretical studies[3] suggest that these interactions can influence essential structural properties of the metal center(s), which, in turn, affect function. For instance, H-bonds involving carboxylate groups are implicated in regulating dioxygen activation in methane monooxygenase,[3] hydrogen atom abstraction in lipoxygenase,[4] and decomposition of superoxide in Fe- and Mn-containing superoxide dismutases.[5]

Efforts to duplicate these structural features in synthetic complexes have proven difficult because H-bonds are relatively weak interactions[6] having a tendency to form intermolecular bonds. Rigid organic frameworks are required to position functional groups near the coordinated ligands in order to facilitate intramolecular H-bonds. Recent relevant examples include an H-bonded η^2-carboxylate in a monomeric Fe^{III}–OH complex and an Fe^{II} dimer with H-bonds to the μ-1,3 carboxylate ligands.[6o,7]

As part of our program on structure–function correlations of synthetic systems with H-bonds,[8] we have developed two new compounds that contain H-bond donors (Fig. 1): bis[(N'-tert-butylureido)-N-ethyl]-2-pyridylmethylamine ($H_4$1) and bis[(N'-tert-butylureido)-N-ethyl]-N-methylamine ($H_4$2).

These ligands are analogues of the symmetrical tripodal compound $H_6$3, whose coordination properties have been previously reported.[8] $H_4$1 is also a tripodal compound, containing two urea-ethylene arms and one pyridylmethylene group distributed around an amine nitrogen atom. $H_4$2 also has a tertiary amine and two urea-ethylene groups—it differs from $H_4$1 by replacement of the pyridylmethylene arm with a methyl group. Deprotonation of the α-NH moieties forms the unsymmetrical

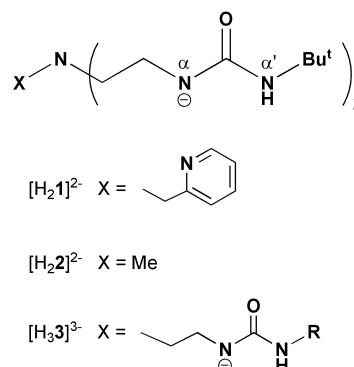**Fig. 1** Multidentate ligands containing H-bond donors.

tripodal ligand $[H_2 1]^{2-}$ and the tridentate ligand $[H_2 2]^{2-}$, both of which provide anionic primary coordination spheres upon binding to a metal ion. Each ligand disposes two α'-NH groups near the metal center, so that formation of intramolecular H-bonds with other coordinated species is possible. Reported herein are the synthesis and structural properties for a series of $[M^{II}(OAc)]^-$ complexes (M^{II} = Fe and Co) of $[H_2 1]^{2-}$ and $[H_2 2]^{2-}$. Our structural studies show that $[H_2 1]^{2-}$ forms complexes with a monodentate coordinated acetato ligand ($[M^{II}(H_2 1)(\eta^1\text{-OAc})]^-$) while those with $[H_2 2]^{2-}$ bind in a bidentate fashion ($[M^{II}(H_2 2)(\eta^2\text{-OAc})]^-$).

Experimental

All reagents and solvents were purchased from commercial sources and used as received, unless noted otherwise. The syntheses of all metal complexes were conducted in a Vacuum Atmosphere drybox under an argon atmosphere. Elemental analyses of all compounds were performed at Desert Analytics, Tucson, AZ. All samples were dried *in vacuo* before analysis. FT-IR and ^1H NMR spectroscopy was used to corroborate the presence of solvates.

† Based on the presentation given at Dalton Discussion No. 5, 10–12th April 2003, Noordwijkerhout, The Netherlands.

Physical methods

Fast atom bombardment mass spectra (FAB-MS) were recorded on a Hewlett-Packard 5989A spectrometer with a HPLC (HP 1050) HP particle-beam interface mass system and a phasor FAB gun. FAB experiments were carried out in a thioglycerol/glycerol (TG/G) matrix and a xenon fast atom beam was used. Fourier transform infrared spectra were recorded on an ATI Mattson Genesis Series FTIR spectrometer, and are reported in wavenumbers. Solid samples were prepared in mineral oil and run between KBr plates. ^{1}H and ^{13}C NMR spectra were recorded on a Bruker 400 MHz spectrometer. Chemical shifts are reported in ppm relative to the internal standard TMS or residual solvent. Electron paramagnetic resonance spectra were collected using a Bruker EMX spectrometer equipped with an ER4102ST cavity. The instrument was previously calibrated using DPPH. Spectrometer settings: microwave frequency, 9.46 GHz; microwave power, 0.638 mW; modulation frequency, 100 kHz and modulation amplitude, 10.02 G. Electronic spectra were collected on a Cary 50 spectrophotometer using 1.00 mm quartz cuvets.

Syntheses

Bis-*N*-(2-phthalimidoethyl)-*N*-(2-pyridylmethyl)amine (4). Bis(2-phthalimidoethyl)amine[9] (20.0 g, 55.1 mmol), picolyl chloride hydrochloride (9.16 g, 55.8 mmol), sodium carbonate (26.2 g, 247 mmol), tetrabutylammonium bromide (0.968 g, 3.00 mmol) and sodium iodide (0.519 g, 3.46 mmol) were dissolved in 350 mL of acetonitrile. The mixture was refluxed with stirring for 24 h, after which time the acetonitrile was removed under reduced pressure and the resulting oil was dissolved in 200 mL each of dichloromethane and brine. The brine solution was washed three times with dichloromethane and the combined dichloromethane solutions were washed three times with brine. The organic solution was dried for 3 h over anhydrous MgSO$_4$ after which time the methylene chloride solution was filtered and evaporated under reduced pressure. The crude product was taken up in a minimum of 8 : 1 EtOAc–MeOH and was passed through a short silica plug until the compound was no longer detectable by TLC (R_f: 0.6, 8 : 1 EtOAc–methanol). The solvent was removed to give an orange–white powder, which was recrystallized from 95% ethanol to give 14.6 g (58.2%) of an off-white solid. δ_H (400 MHz; solvent CDCl$_3$): 8.41 (1 H, d, *J* 4.7 Hz, PyH), 7.71 (8 H, s, Phth-*H*), 7.08 (2 H, m, PyH), 7.00 (1 H, m, PyH), 3.86 (2 H, s, N–CH$_2$–Py), 3.79 (4 H, t, *J* 6.1 Hz, CH$_2$–CH$_2$–Phth), 2.86 (4 H, t, *J* 6.1 Hz, N–CH$_2$–CH$_2$). δ_C (400 MHz; solvent CDCl$_3$): 168.50, 159.60, 149.08, 136.42, 134.04, 132.34, 123.48, 122.24, 60.20, 52.31, 36.03. FT-IR/cm^{-1} (Nujol): $\tilde{v}$ 1769s, 1590m, 1465s, 1449s, 1399s, 1371s, 1327m, 1187m, 1096s, 1085s, 1045m, 988m, 906m, 843w, 795m, 775m, 723s, 611w, 529m, 468w, 411w. Mp 106–108 °C. *m/z* 455.2 (FAB$^+$, TG/G + MeOH matrix).

Bis[(*N'*-*tert*-butylureido)-*N*-ethyl]-*N*-pyridylmethylamine (H$_4$1). Bis-*N*-(2-phthalimidoethyl)-*N*-(2-pyridylmethyl)amine (**4**) (5.68 g, 12.5 mmol) and hydrazine hydrate (6.23 g, 124.5 mmol) were dissolved in 200 mL of ethanol and heated at reflux overnight. The reaction mixture was allowed to cool to room temperature and filtered to remove a white precipitate. Ethanol was removed under reduced pressure to give an orange oil, which is the free amine [CDCl$_3$, δ 8.31 (d, 1 H, Py–*H*), 7.69 (t, 1 H, Py–*H*), 7.30 (d, 1 H, Py–*H*), 7.22 (t, 1 H, Py–*H*), 3.57 (s, 2 H, Py–C*H*$_2$–N), 2.60 (t, 4 H, CH$_2$–C*H*$_2$–NH$_2$), 2.43 (t, 4 H, N–C*H*$_2$–CH$_2$)]. This oil was suspended in 100 mL anhydrous THF under a N$_2$ atmosphere and *tert*-butyl isocyanate (2.66 g, 26.8 mmol) was added slowly. The reaction was allowed to stir overnight to form a suspension of white powder. Solvent was removed under reduced pressure to give an off-white solid, which was subsequently crystallized from methanol layered with diethyl ether at −20 °C to give pure white crystalline com-

pound (3.65 g, 74.4%). δ_H (400 MHz; solvent DMSO-*d*$_6$): 8.48 (1 H, d, *J* 4.3 Hz, PyH), 7.62 (1 H, t of d, *J* 7.7, 1.8 Hz, PyH), 7.43 (1 H, d, *J* 7.8 Hz, PyH), 7.15 (1 H, d, *J* 6.0, PyH), 5.81 (2 H, s, CH2–NH–CO), 5.11 (2 H, s, CO–NH–*t*Bu), 3.70 (1 H, s, N–CH$_2$–Py), 3.14 (4 H, t, *J* 4.6 Hz, CH$_2$–CH$_2$–NH), 2.53 (4 H, t, *J* 5.0 Hz, N–CH$_2$–CH$_2$), 1.34 (18 H, s, *t*BuH). δ_C (400 MHz; solvent CDCl$_3$): 160.34, 158.93, 149.04, 136.89, 123.91, 122.49, 61.49, 56.12, 50.36, 38.28, 30.07. FT-IR/cm^{-1} (Nujol): $\tilde{v}$ 3367s, 3267s (NH), 1631s, 1570s, 1457s, 1360s, 1282s, 1217s, 1146m, 1062w, 992w, 753m, 651m, 534w. Mp 141–144 °C. *m/z* 393.3 (FAB$^+$, TG/G + MeOH matrix).

Bis[(*N'*-*tert*-butylureido)-*N*-ethyl]-*N*-methylamine (H$_4$2). *N'*-Methyl-2,2'-diaminodiethylamine (5.04 g, 0.0430 mmol) was dissolved in 75 mL of anhydrous THF under a nitrogen atmosphere. 2.1 eq. of *tert*-butyl isocyanate (9.02 g, 0.0910 mmol) was added slowly. After addition, the solution was allowed to stir at room temperature overnight. The solution was filtered and the precipitate was washed with diethyl ether before oven-drying overnight to yield 13.04 g (96.2%) of white precipitate. δ_H (400 MHz; solvent DMSO-*d*$_6$): 5.72 (2 H, s, CO–NH–*t*Bu), 5.59 (2 H, t, *J* 5.3, CH$_2$–NH–CO), 3.02 (4 H, q, *J* 5.9, CH$_2$–CH$_2$–NH), 2.31 (4 H, t, *J* 6.3, N–CH$_2$–CH$_2$), 2.16 (3 H, s, MeH), 1.22 (18 H, s, *t*BuH). δ_C (400 MHz; solvent DMSO-*d*$_6$): 158.21, 57.77, 49.79, 42.89, 37.57, 30.19. FT-IR/cm^{-1} (Nujol): $\tilde{v}$ 3381s, 3351s, 3308s, 3178w, 3122w, 1631s, 1560s, 1377s, 1362m, 1292m, 1270m, 1222m, 1207m, 1157m, 1122w, 1047w, 969w, 937w, 772w, 676w, 639w, 425w. Mp 187–189 °C. *m/z* 316.2 (FAB$^+$, TG/G + MeOH matrix).

K[Fe^{II}(H$_2$1)(η^1-OAc)]. A solution of H$_4$1 (182 mg, 0.464 mmol) in anhydrous *N,N*-dimethylacetamide (DMA, 10 mL) was treated with solid KH (37 mg, 0.92 mmol) under an Ar atmosphere. After gas evolution ceased, solid Fe(OAc)$_2$ (81 mg, 0.47 mmol) was added slowly. The resulting purple–red solution was stirred for 1 h and then filtered to remove insoluble KOAc (47 mg, 0.48 mmol). Diethyl ether vapor was allowed to diffuse into the filtrate to afford K[(H$_2$1)Fe^{II}(η^1-OAc)] as a red powder (204 mg, 80.7% yield). Found: C, 48.29; H, 7.10; N, 15.09. K[(H$_2$1)Fe^{II}(η^1-OAc)] (C$_{22}$H$_{37}$FeKN$_6$O$_4$) requires C, 48.52; H, 6.86; N, 15.44%. FT-IR/cm^{-1} (Nujol): $\tilde{v}$ 3412w, 3356s (NH), 1647m, 1623s, 1585s, 1506s, 1457s, 1377s, 1321s, 1245m, 1213m, 1153w, 1134w, 1045w, 917w, 650w. λ_{max}/nm (DMA, ε/mol dm^{-3} cm^{-1}): 512 (350). *g* = 9.85 (DMA, 4 K).

K[Co^{II}(H$_2$1)(η^1-OAc)]. Synthesized by the same route as K[(H$_2$1)Fe^{II}(η^1-OAc)] using H$_4$1 (204 mg, 0.520 mmol) and Co(OAc)$_2$ (93 mg, 0.525 mmol). The compound was purified by recrystallization with DMA and ether to yield a purple solid (214 mg, 75.1% yield). Found: C, 46.60; H, 7.03; N, 14.54. K[Co^{II}(H$_2$1)(η^1-OAc)] (C$_{22}$H$_{37}$CoKN$_6$O$_4$) requires C, 48.24; H, 6.82; N, 15.34%. Repeated elemental analysis gave consistently low values. FT-IR/cm^{-1} (Nujol): $\tilde{v}$ 3400w, 3338w (NH), 1647m, 1622m, 1584s, 1507s, 1457s, 1377s, 1334s, 1322s, 1245s, 1212s, 1154m, 1136w, 1059m, 1044m, 1016w, 917w, 894w, 786w, 769w, 724w, 651w, 614w, 593w, 558w, 523w, 481w. λ_{max}/nm (DMA, ε/mol dm^{-3} cm^{-1}): 314 (2200), 490sh (44), 566 (150). *g* = 5.52, 3.02, 1.88 (DMA, 4 K).

K[Fe^{II}(H$_2$2)(η^2-OAc)]. A solution of H$_4$2 (314 mg, 0.995 mmol) in anhydrous *N,N*-dimethylacetamide (DMA, 10 mL) was treated with solid KH (81 mg, 2.0 mmol) under an Ar atmosphere. After gas evolution ceased, solid Fe(OAc)$_2$ (172 mg, 0.99 mmol) was added slowly. The resulting light tan solution was stirred for 1 h and then filtered to remove insoluble KOAc (101 mg, 1.02 mmol). Diethyl ether vapor was allowed to diffuse into the filtrate to afford K[(H$_2$2)Fe^{II} (η^2-OAc)] as a white powder (379 mg, 81.5% yield). Found: C, 43.63; H, 7.58; N, 14.39. K[(H$_2$2)Fe^{II}(η^2-OAc)] (C$_{17}$H$_{34}$FeKN$_5$O$_4$) requires C, 43.67; H, 7.35; N, 14.99%. FT-IR/cm^{-1} (Nujol): $\tilde{v}$ 3394sh,

Complex	K[Fe^{II}(H$_2$**1**)(η^1-OAc)]·DMA	K[Co^{II}(H$_2$**1**)(η^1-OAc)]·0.93DMA·0.07H$_2$O	K[Fe^{II}(H$_2$**2**)(η^2-OAc)]	K[Co^{II}(H$_2$**2**)(η^2-OAc)]·DMA
Empirical formula	C$_{26}$H$_{46}$FeKN$_7$O$_5$	C$_{25.72}$H$_{45.51}$CoKN$_{6.93}$O$_5$	C$_{17}$H$_{34}$FeKN$_5$O$_4$	C$_{21}$H$_{43}$CoKN$_6$O$_5$
FW	631.95	629.89	467.44	557.64
T/K	173(2)	100(2)	100(2)	100(2)
Crystal system	Triclinic	Triclinic	Triclinic	Monoclinic
Space group	$P\bar{1}$	$P\bar{1}$	$P\bar{1}$	$P2_1/n$
a/Å	10.339(3)	10.2758(14)	10.4396(6)	16.3720(9)
b/Å	11.171(4)	11.0982(15)	15.1673(9)	11.1959(6)
c/Å	14.453(5)	14.4052(19)	17.0455(10)	16.8233(9)
α/°	79.414(7)	78.561(3)	70.427(2)	90
β/°	82.092(7)	82.114(3)	74.547(2)	113.305(2)
γ/°	86.388(7)	85.728(3)	70.066(2)	90
Z	2	2	4	4
V/Å^3	1624.1(9)	1593.1(4)	2355.1(2)	2832.1(3)
μ_{calc}/mm^{-1}	0.636	0.713	0.847	0.792
F(000)	672	669	992	1188
Crystal dimensions/mm	0.16 × 0.15 × 0.03	0.38 × 0.20 × 0.10	0.27 × 0.23 × 0.13	0.28 × 0.26 × 0.14
Radiation	Mo-Kα ($\lambda = 0.71073$ Å)	Mo-Kα ($\lambda = 0.71073$ Å)	Mo-Kα ($\lambda = 0.71073$ Å)	Mo-Kα ($\lambda = 0.71073$ Å)
No. of reflections collected	9994	13274	19279	23078
No. of independent	5634 ($R_{int} = 0.0499$)	8448 ($R_{int} = 0.0163$)	12406 ($R_{int} = 0.0190$)	8252 ($R_{int} = 0.0198$)
No. of parameters	371	391	505	362
R^a	0.0798	0.0411	0.0531	0.0444
$R_w{}^b$	0.1474	0.1091	0.1381	0.1302
GOF^c	1.037	1.028	1.107	1.060

^{a} $R = [\Sigma|\Delta F|/\Sigma|F_o|]$. ^{b} $R_w = [\Sigma\omega(\Delta F)^2/\Sigma\omega F_o^2]$. ^{c} Goodness of fit on F^2.

3379s, 3166w (NH), 1602s, 1577s, 1554s, 1504s, 1504s, 1377s, 1343s, 1323s, 1249s, 1216s, 1147m, 1126m, 1072m, 1045m, 1002m, 938m, 913m, 893m, 785m, 671m, 618m, 556m, 429m. g = 7.34 (DMA, 4 K).

K[Co^{II}(H$_2$2)(η^2-OAc)]. Synthesized by the same route as K[(H$_2$2)Fe^{II}(η^2-OAc)] using H$_4$2 (288 mg, 0.913 mmol) and Co(OAc)$_2$ (162 mg, 0.915 mmol). The compound was purified by recrystallization from DMA and ether, to yield a light purple solid (340 g, 79.1% yield). Found: C, 42.20; H, 6.77; N, 13.00. K[(H$_2$2)Co^{II}(η^2-OAc)] (C$_{17}$H$_{34}$CoKN$_5$O$_4$) requires C, 43.39; H, 7.30; N, 14.89%. Repeated elemental analysis gave consistently low values. FT-IR/cm^{-1} (Nujol): $\tilde{\nu}$ 3389m, 3364m, 3167w (NH), 1600s, 1573s, 1508s, 1378s, 1358s, 1342s, 1322s, 1250m, 1217m, 1147m, 1125m, 1073m, 1045m, 1004m, 936m, 915m, 894m, 788m, 672m, 621m, 559m, 431m. λ_{max}/nm (DMA, ε/mol dm^{-3} cm^{-1}) 306 (3800), 438 (100), 565 (90). g = 9.08, 5.08, 3.64, 1.88 (DMA, 4 K).

Crystallographic structural determination

Crystal data collection, and refinement parameters for K[Fe(H$_2$1)(η^1-OAc)]·DMA, K[Co^{II}(H$_2$1)(η^1-OAc)]·0.93DMA·0.07H$_2$O, K[Fe^{II}(H$_2$2)(η^2-OAc)], and K[Co(H$_2$2)(η^2-OAc)]·DMA are given in Table 1. For all the structures, the non-hydrogen atoms were refined with anisotropic displacement parameters. All hydrogen atoms were placed in ideal positions and refined as riding atoms with relative isotropic displacement parameters. For K[Fe(H$_2$1)(η^1-OAc)]·DMA, there are two ~1e peaks in the neighborhood of the DMA, which may indicate that this is compositionally disordered in some way. No attempt was made to model any hypothetical disorder. For K[Co^{II}(H$_2$1)(η^1-OAc)]·0.93DMA·0.07H$_2$O, the solvent region was disordered and modeled with two orientations of DMA and one position for water. The occupancies of the DMA refined to 0.846(3) and 0.083(3) for the unprimed and primed atoms; the occupancy of the water refined to 0.070(2). Restraints on the positional parameters of the DMA were required. For K[Co(H$_2$2)(η^2-OAc)] the DMA solvent was disordered and modeled in two orientations with refined occupancies of 0.706(5) and 0.294(5) for the unprimed and

primed atoms. Restraints on the positional and displacement parameters of the DMA atoms were required.

Results and discussion

Ligand design and synthesis

Ligands [H$_2$**1**]$^{2-}$ and [H$_2$**2**]$^{2-}$ are formed by deprotonation of the α nitrogen atoms on the urea groups, leading to dianionic ligands that readily bind metal ions. The remaining components of the ureas are thus positioned such that the two α'-NHR groups are proximal to the coordinated metal ion. The relatively rigid urea groups promote intramolecular H-bonds between the α'-NHR groups and an atom coordinated to the metal center— these interactions are favored thermodynamically because six-membered rings are formed. Complexes of [H$_2$**1**]$^{2-}$ and [H$_2$**2**]$^{2-}$ should have more exposed metal centers compared to those found for the parent ligand [H$_3$**3**]$^{3-}$, which has three urea-ethylene arms. The less constrained secondary coordination spheres in complexes with these new ligands, coupled with the decrease in H-bond donors, should lead to different binding properties.

The synthesis of H$_4$**1** is outlined in Scheme 1. Installation of the pyridylmethylene arm was accomplished by treating bis-(2-phthalimidoethyl)amine with picolyl chloride hydrochloride under basic conditions to afford **4** in 58% yield. Allowing **4** to react with hydrazine hydrate gave the pyridyl-diamine compound, which, without purification, is reacted with *tert*-butyl isocyanate to produce H$_4$**1** in a yield of 74%. H$_4$**2** was prepared in 96% yield by treating N'-methyl-2,2'-diaminodiethylamine with *tert*-butyl isocyanate (Scheme 2).

Deprotonation of H$_4$**1** and H$_4$**2** was achieved with KH. After gas evolution ceased, the appropriate M^{II}(OAc)$_2$ precursor was added to produce the potassium salts of [M^{II}(H$_2$**1**)(η^1-OAc)]$^-$ and [M^{II}(H$_2$**2**)(η^2-OAc)]$^-$ in yields ranging from 50 to 80%. One equivalent of potassium acetate also was isolated for each metallation reaction. Solid state samples of these salts were stable for weeks under a dry, anaerobic environment.
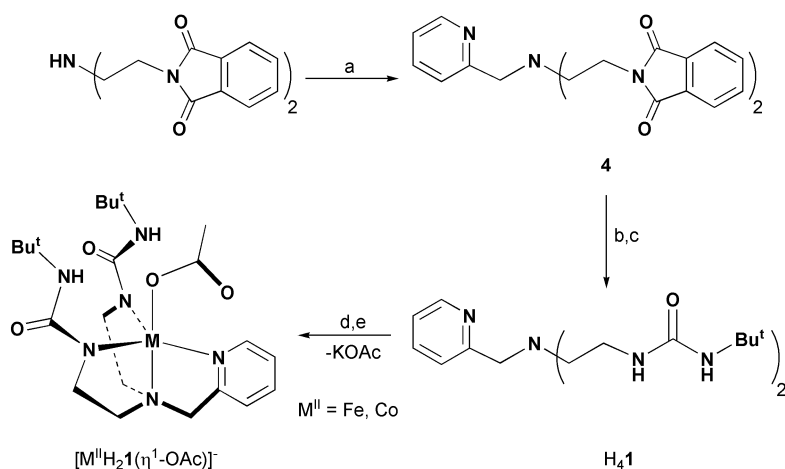
Scheme 1 Reagents and conditions: (a) picolyl chloride hydrochloride, Na$_2$CO$_3$, Bu$_4$NBr, NaI, ACN, ↑↓N$_2$; (b) N$_2$H$_4$·H$_2$O, EtOH, N$_2$; (c) 2.1 equiv. OCN[C(CH$_3$)$_3$], THF, ↑↓N$_2$; (d) 2 equiv. KH, DMA, rt, Ar; (e) M^{II}(OAc)$_2$, DMA, rt, Ar.
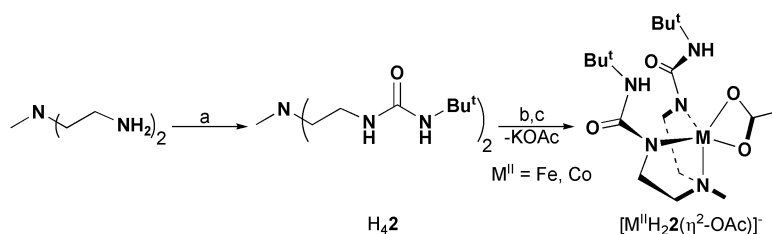
Scheme 2 Reagents and conditions: (a) 2.1 equiv. OCN[C(CH$_3$)$_3$], THF, N$_2$; (b) 2 equiv. KH, DMA, rt, Ar; (c) M^{II}(OAc)$_2$, DMA, rt, Ar.

Table 2 Selected bond distances (Å) and angles (°) for [Fe^{II}(H$_2$1)(η^1-OAc)]$^-$ and [Co^{II}(H$_2$1)(η^1-OAc)]$^-$

	[Fe^{II}(H$_2$1)(η^1-OAc)]$^-$	[Co^{II}(H$_2$1)(η^1-OAc)]$^-$
M–N1	2.260(6)	2.2014(14)
M–N4	2.028(6)	1.9982(13)
M–N14	2.048(6)	2.0056(14)
M–N24	2.207(6)	2.1383(14)
M–O29	2.072(5)	2.0849(12)
N7 ··· O29	3.220(8)	3.0578(18)
N17 ··· O29	2.924(8)	2.8553(18)
N1–M–N4	80.0(2)	81.01(5)
N1–M–N14	80.7(2)	82.43(5)
N1–M–N24	75.3(2)	76.91(5)
N1–M–O29	166.2(2)	169.56(5)
N4–M–N14	114.3(2)	117.22(6)
N4–M–N24	125.5(2)	124.52(6)
N4–M–O29	109.6(2)	105.12(5)
N14–M–N24	108.6(2)	109.42(5)
N24–M–O29	90.9(2)	92.65(5)

Molecular structure results

Single crystal X-ray diffraction studies were done on K[Fe^{II}-(H$_2$1)(η^1-OAc)]·DMA, K[Co^{II}(H$_2$1)(η^1-OAc)]·0.93DMA·0.07-H$_2$O, K[Fe^{II}(H$_2$2)(η^2-OAc)], and K[Co(H$_2$2)(η^2-OAc)]·DMA. Crystal, data collection, and refinement parameters are given in Table 1. Selected distances and angles for [Fe^{II}(H$_2$1)(η^2-OAc)]$^-$ and [Co^{II}(H$_2$1)(η^1-OAc)]$^-$ are presented in Table 2 while those for [Fe^{II}(H$_2$2)(η^2-OAc)]$^-$ and [Co^{II}(H$_2$2)(η^2-OAc)]$^-$ are found in Table 3. For K[Fe^{II}(H$_2$2)(η^2-OAc)], two independent but virtually identical anions were found in the asymmetric unit, denoted [Fe^{II}(H$_2$2a)(η^2-OAc)]$^-$ and [Fe^{II}(H$_2$2b)(η^2-OAc)]$^-$.

The molecular structures of [Fe^{II}(H$_2$1)(η^1-OAc)]$^-$ and [Co^{II}-(H$_2$1)(η^1-OAc)]$^-$ are shown in Fig. 2. Each complex has a trigonal bipyramidal coordination geometry: the index for the degree of trigonality [10] (τ) for [Fe^{II}(H$_2$1)(η^1-OAc)]$^-$ is 0.69, while that for [Co^{II}(H$_2$1)(η^1-OAc)]$^-$ is 0.75. The trigonal plane is defined by the two deprotonated urea nitrogen atoms N4 and N14, and the pyridyl nitrogen atom N24. The M–N$_{urea}$ dis-
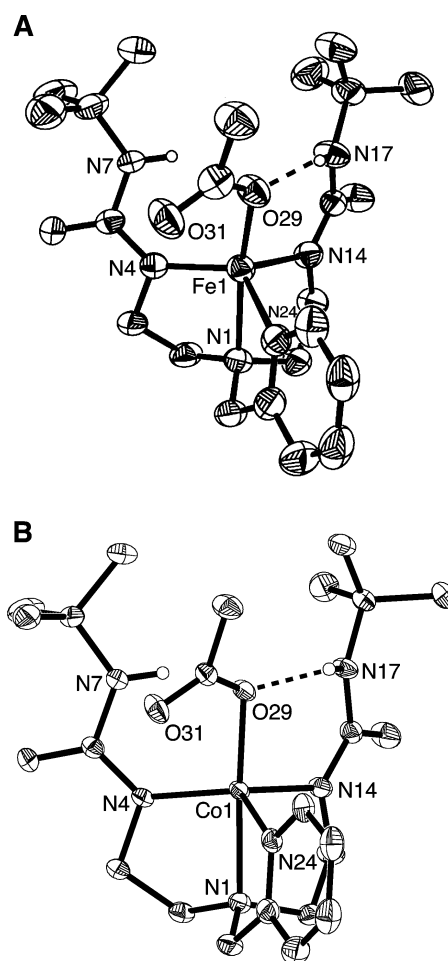
Fig. 2 Thermal ellipsoid plots of [Fe^{II}(H$_2$1)(η^1-OAc)]$^-$ (**A**) and [Co^{II}(H$_2$1)(η^1-OAc)]$^-$ (**B**). Thermal ellipsoids are drawn at the 50% probability level and only urea hydrogens are shown. Dashed lines indicate H-bonds.

Table 3 Selected bond distances (Å) and angles (°) for $[Fe^{II}(H_2\mathbf{2})(\eta^2\text{-OAc})]^-$ and $[Co^{II}(H_2\mathbf{2})(\eta^2\text{-OAc})]^{-\,a}$

	$[Fe^{II}(H_2\mathbf{2})(\eta^2\text{-OAc})]^-$		$[Co^{II}(H_2\mathbf{2})(\eta^2\text{-OAc})]^-$
	$[Fe^{II}(H_2\mathbf{2a})(\eta^2\text{-OAc})]^-$	$[Fe^{II}(H_2\mathbf{2b})(\eta^2\text{-OAc})]^-$	
M–N1	2.207(2)	2.206(2)	2.1160(15)
M–N4	2.010(2)	2.019(2)	1.9642(15)
M–N14	2.037(2)	2.023(2)	1.9570(15)
M–O23	2.1600(9)	2.155(2)	2.0278(13)
M–O25	2.284(2)	2.272(2)	2.4436(4)
N7 ⋯ O25	3.005(3)	3.071(3)	3.008(2)
N17 ⋯ O25	2.957(3)	2.894(3)	3.001(2)
N1–M–N4	83.70(9)	82.69(8)	85.02(6)
N1–M–N14	82.28(8)	83.09(8)	85.00(6)
N1–M–O23	107.41(8)	106.49(8)	103.08(6)
N1–M–O25	164.90(8)	163.80(8)	161.39(5)
N4–M–N14	127.00(9)	123.08(9)	121.28(6)
N4–M–O23	105.81(8)	106.69(8)	119.64(6)
N4–M–O25	105.59(8)	107.83(8)	102.39(6)
N14–M–O23	127.17(8)	130.20(9)	119.00(6)
N14–M–O25	100.64(8)	100.40(8)	104.92(5)
O23–M–O25	58.97(8)	59.19(7)	58.38(5)

^{a} There are two independent anions in the asymmetric unit for the $[Fe(H_2\mathbf{2})(\eta^2\text{-OAc})]^-$ complex. Metric parameters for both are reported.

tances in $[Fe^{II}(H_2\mathbf{1})(\eta^1\text{-OAc})]^-$ and $[Co^{II}(H_2\mathbf{1})(\eta^1\text{-OAc})]^-$ are similar to those observed for other five-coordinate Co^{II} and Fe^{II} complexes with deprotonated urea donors.[8a,c,d] All the N–M–N angles within the basal plane deviate from the expected 120° for trigonal symmetry. For example, N4–M–N24 angles of 125.5(2) and 124.52(6)° are found in $[Fe^{II}(H_2\mathbf{1})(\eta^1\text{-OAc})]^-$ and $[Co^{II}(H_2\mathbf{1})(\eta^1\text{-OAc})]^-$, respectively. This enlarged angle is probably caused by the proximity of the acetato ligand. Similarly enlarged angles were observed in the trigonal plane of M^{II}–OH complexes with the tripodal ligand $[H_3\mathbf{3}]^{3-}$.[8a,c,d] The apical nitrogen atom N1 sits approximately perpendicular to the trigonal plane and is positioned nearly *trans* to O29 of the acetato ligand; the N1–M1–O29 angle in $[Co^{II}(H_2\mathbf{1})(\eta^1\text{-OAc})]^-$ is 169.56(5)°, while in $[Fe^{II}(H_2\mathbf{1})(\eta^1\text{-OAc})]^-$ it is 166.2(2)°.

Fig. 3 contains the molecular structures of $[Fe^{II}(H_2\mathbf{2})(\eta^2\text{-OAc})]^-$ and $[Co^{II}(H_2\mathbf{2})(\eta^2\text{-OAc})]^-$. The coordination geometry in these complexes is best described as trigonal bipyramidal with τ values of 0.62 and 0.56 for $[Fe^{II}(H_2\mathbf{2a})(\eta^2\text{-OAc})]^-$ and $[Fe^{II}(H_2\mathbf{2b})(\eta^2\text{-OAc})]^-$ and 0.67 for $[Co^{II}(H_2\mathbf{2})(\eta^2\text{-OAc})]^-$. The trigonal plane is composed of N4 and N14 of $[H_2\mathbf{2}]^{2-}$ and O23 of the acetato ligand. Nearly all the Fe–N_{urea} distances in $[Fe^{II}(H_2\mathbf{2})(\eta^2\text{-OAc})]^-$ are statistically same as those found in $[Fe^{II}(H_2\mathbf{1})(\eta^1\text{-OAc})]^-$—only the Fe1a–N4a distance at 2.010(2) Å is outside the statistical limit.[11] For $[Co^{II}(H_2\mathbf{2})(\eta^2\text{-OAc})]^-$, the average Co–N_{urea} distance is 0.041 Å shorter than that found in $[Co^{II}(H_2\mathbf{1})(\eta^1\text{-OAc})]^-$. Shorter M–N1 distances are also observed in $[Fe^{II}(H_2\mathbf{2})(\eta^2\text{-OAc})]^-$ and $[Co^{II}(H_2\mathbf{2})(\eta^2\text{-OAc})]^-$ compared to those in the M^{II}–OAc complexes of $[H_2\mathbf{1}]^-$. These shorter distances may reflect the positioning of the O25 donor in the two $[M^{II}(H_2\mathbf{2})(\eta^2\text{-OAc})]^-$ complexes, whose N1–M1–O25 angles are less than 165°, which are significantly smaller than those in $[M^{II}(H_2\mathbf{1})(\eta^1\text{-OAc})]^-$ (*vide supra*).

The acetato ligands in $[Fe^{II}(H_2\mathbf{1})(\eta^1\text{-OAc})]^-$ and $[Co^{II}(H_2\mathbf{1})(\eta^1\text{-OAc})]^-$ bind in a monodentate manner, with Fe1–O29 and Co1–O29 distances of 2.072(5) and 2.0849(12) Å, respectively. A CSD[12] search reveals that M–O distances range from 2.02–2.14 and 1.91–2.11 Å for Fe^{II}-$(\eta^1\text{-OAc})$[13] and Co^{II}-$(\eta^1$-OAc)[14] complexes, respectively. The finding that this distance in $[Fe^{II}(H_2\mathbf{1})(\eta^1\text{-OAc})]^-$ and $[Co^{II}(H_2\mathbf{1})(\eta^1\text{-OAc})]^-$ is near the higher end of these ranges reflects the presence of intramolecular H-bonds to O29 (*vide infra*). Note that previously reported Co^{II}-$(\eta^1$-OAc) complexes with Co–O ⋯ H–X interactions also have relatively long metal–oxygen distances. For example, a Co–O distance of 2.070(4) Å is observed for the [Co(biap)(OAc)(NCS)] complex [biap, *N,N*-bis(2-ethyl-5-methylimidazol-4-ylmethyl)aminopropane],[15] which has one
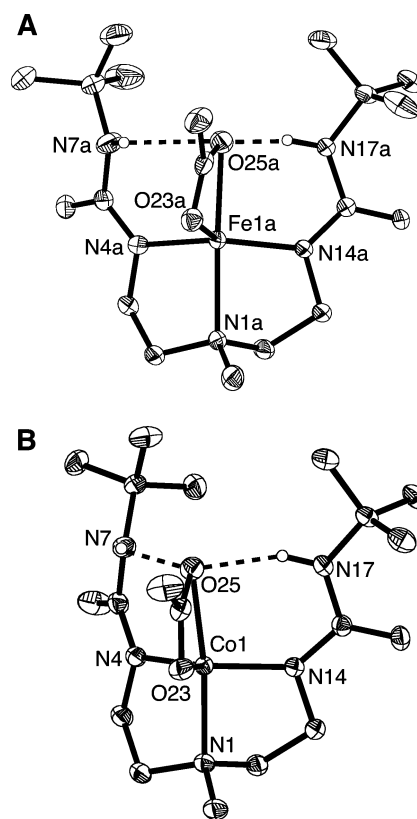
Fig. 3 Thermal ellipsoid plots of $[Fe^{II}(H_2\mathbf{2})(\eta^2\text{-OAc})]^-$ (**A**) and $[Co^{II}(H_2\mathbf{2})(\eta^2\text{-OAc})]^-$ (**B**). Thermal ellipsoids are drawn at the 50% probability level and only urea hydrogens are shown. Dashed lines indicate H-bonds.

intramolecular H-bond to each coordinated acetato oxygen atom. The Fe1 and Co1 distances to the other acetato oxygen atom, O31 in $[Fe^{II}(H_2\mathbf{1})(\eta^1\text{-OAc})]^-$ and $[Co^{II}(H_2\mathbf{1})(\eta^1\text{-OAc})]^-$ are 3.158(5) and 3.182(1) Å, which are too long for bonding interactions. However O31 does interact with the potassium counterion: the observed K1 ⋯ O31 distances are 2.774(6) ($[Fe^{II}(H_2\mathbf{1})(\eta^1\text{-OAc})]^-$) and 2.7437(13) Å ($[Co^{II}(H_2\mathbf{1})(\eta^1\text{-OAc})]^-$). In addition, K1 is chelated to O6, a ureido oxygen atom on the $[H_2\mathbf{1}]^-$ ligand. Distances for this K1 ⋯ O6 interaction are 2.599(5) and 2.5862(12) Å in $[Fe^{II}(H_2\mathbf{1})(\eta^2\text{-OAc})]^-$ and $[Co^{II}(H_2\mathbf{1})(\eta^1\text{-OAc})]^-$, respectively.

In $[Fe^{II}(H_21)(\eta^2\text{-OAc})]^-$ and $[Co^{II}(H_22)(\eta^2\text{-OAc})]^-$ the acetate coordinates as an unsymmetrical bidentate ligand. The longer M–O distance involves the apical oxygen atom, O25, with average Fe1–O25 distances being greater than 0.1 Å that found for Fe1–O23. This difference in bond lengths is larger in $[Co^{II}(H_22)(\eta^2\text{-OAc})]^-$ where the Co1–O25 and Co1–O23 distances are at 2.4436(14) and 2.0278(13) Å. Although large differences in M–O bond lengths are not unusual for bidentate carboxylate ligation, both long M–O distances in $[Fe^{II}(H_22)(\eta^2\text{-OAc})]^-$ and $[Co^{II}(H_22)(\eta^2\text{-OAc})]^-$ involve O25, which also participates in H-bonding.

Intramolecular H-bonds

As discussed above, all the M^{II}–OAc complexes have intramolecular H-bonds, which arise from α'-NH $\cdots$ O–M interactions. The two urea groups present in the $[H_21]^{2-}$ and $[H_22]^-$ ligands form a partial H-bond cavity, which encompasses the M–O unit. For $[Fe^{II}(H_21)(\eta^1\text{-OAc})]^-$, an N17 $\cdots$ O29 distance and N17–H–O29 angle of 2.924(8) and 153.8(4)° are consistent with intramolecular H-bonds. Similar metrical parameters are found for $[Co^{II}(H_21)(\eta^1\text{-OAc})]^-$: N17 $\cdots$ O29, 2.8553(18); N17–H–O29, 146.6(7)°. Longer N7 $\cdots$ O29 distances and reduced N7–H–O29 angles are observed in both complexes, suggesting weaker interactions. In $[Fe^{II}(H_21)(\eta^1\text{-OAc})]^-$, the N7 $\cdots$ O29 distance is 3.220(8) and the N7–H–O29 angle is 121.5°, while in $[Co^{II}(H_21)(\eta^1\text{-OAc})]^-$ these metrical parameters are 3.0578(18) Å and 119.0°.

The parameters for the intramolecular H-bonds observed for $[Fe^{II}(H_22)(\eta^2\text{-OAc})]^-$ and $[Co^{II}H_22(\eta^2\text{-OAc})]^-$ suggest more symmetrical interactions than those found in the complexes with $[H_21]^-$. In $[Fe^{II}(H_22a)(\eta^2\text{-OAc})]^-$ and $[Co^{II}(H_22)(\eta^2\text{-OAc})]^-$ the difference between the N7 $\cdots$ O25 and N17 $\cdots$ O25 distance are less than 0.05 Å, while in $[Fe^{II}(H_22b)(\eta^2\text{-OAc})]^-$ this difference in H-bond length is 0.177 Å. In addition, the deviations between the N7–H–O25 and N17–H–O25 angles are smaller, ranging from 1.8° in $[Co^{II}(H_22)(\eta^2\text{-OAc})]^-$ to 20° in $[Fe^{II}(H_22a)(\eta^2\text{-OAc})]^-$.

Results from solid-state FT-IR measurements support the existence of different H-bonds in these complexes (Fig. 4). The FT-IR spectrum for $[Fe^{II}(H_21)(\eta^1\text{-OAc})]^-$ contains two peaks at 3412 and 3356 cm^{-1}, which are assigned to the NH vibrations of $[H_21]^{2-}$ (Fig. 4A). Comparable signals are observed in the spectrum of $[Co^{II}(H_21)(\eta^1\text{-OAc})]^-$ at 3400 and 3338 cm^{-1}. Two peaks are also found in the FT-IR spectra of $[Fe^{II}(H_22)(\eta^2\text{-OAc})]^-$ and $[Co^{II}(H_22)(\eta^2\text{-OAc})]^-$ (Fig. 4B) but their energies are more comparable. For $[Fe^{II}(H_22)(\eta^2\text{-OAc})]^-$ the $\tilde{\nu}$(NH) signals appear as a shoulder at 3394 and a peak at 3379 cm^{-1}, while in $[Co^{II}(H_22)(\eta^2\text{-OAc})]^-$ they are at 3389 and 3364 cm^{-1}. The similarity in energies of these signals supports the assignment of a more symmetrical H-bond network in $[Fe^{II}(H_22)(\eta^2\text{-OAc})]^-$ and $[Co^{II}(H_22)(\eta^2\text{-OAc})]^-$.

Summary and conclusions

We have presented two new multidentate ligands $[H_21]^{2-}$ and $[H_22]^{2-}$, which contain H-bond donors from two urea groups. These ligands are analogues of $[H_33]^{3-}$, the symmetrical tripodal ligand containing three urea-ethylene arms (Fig. 1). The replacement of one of these arms in $[H_33]^{3-}$ with either a pyridylmethylene group ($[H_21]^{2-}$) or a methyl group ($[H_22]^{2-}$) yields ligands whose complexes have more exposed metal centers than those with $[H_33]^{3-}$. Thus both $[H_21]^{2-}$ and $[H_22]^{2-}$ form monomeric M^{II}–OAc complexes (M^{II} = Fe, Co), whereas we have been unsuccessful in isolating similar acetate complexes with $[H_33]^{3-}$. $[M^{II}(H_21)(\eta^1\text{-OAc})]^-$ and $[M^{II}(H_22)(\eta^2\text{-OAc})]^-$ differ in their mode of acetate coordination: $[M^{II}(H_21)(\eta^1\text{-OAc})]^-$ complexes have a monodentate coordination, whereas in $[M^{II}(H_22)(\eta^2\text{-OAc})]^-$ the acetate binds in a bidentate manner. All the complexes have intramolecular H-bonds involving urea

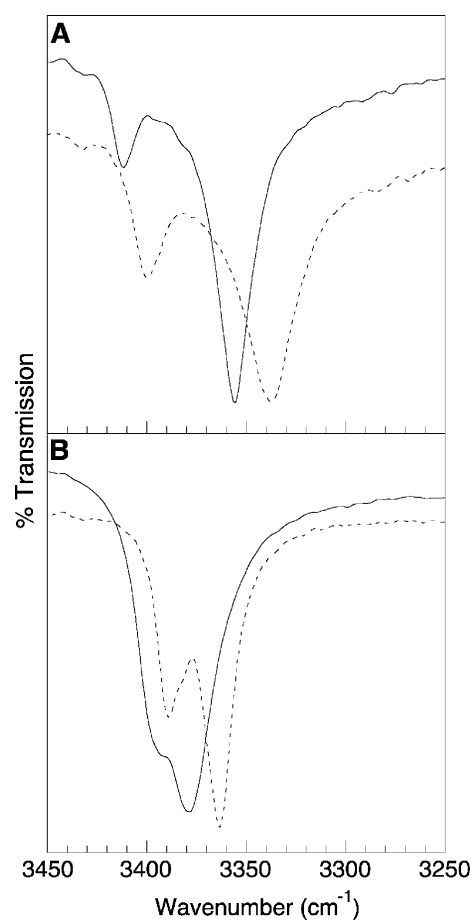**Fig. 4** Solid-state FT-IR spectra of $[Fe^{II}(H_21)(\eta^1\text{-OAc})]^-$ and $[Co^{II}(H_21)(\eta^1\text{-OAc})]^-$ (**A**) and $[Fe^{II}(H_22)(\eta^2\text{-OAc})]^-$ and $[Co^{II}(H_22)(\eta^2\text{-OAc})]^-$ (**B**). The spectra of the iron complexes are represented with a solid line and those of the cobalt complexes are dashed.

α'-NH groups of the ligands and the acetate oxygen atom that is coordinated to the metal center. Examples of this type of H-bond in complexes with monodentate acetates are rare, where H-bonds to the uncoordinated acetate oxygen atom are more typical. We attribute the H-bonding in $[M^{II}(H_21)(\eta^1\text{-OAc})]^-$ complexes to the formation of a partial H-bond cavity, which is rigid and disposes the α'-NH groups to favor interactions with the coordinated oxygen atom.

Results from X-ray diffraction and FT-IR measurements are consistent with the formation of $[M^{II}(H_22)(\eta^2\text{-OAc})]^-$ complexes forming a more symmetrical H-bond network around the metal aceteto unit. However, within the crystal lattices the potassium counterions interact with each anion. In $[M^{II}(H_22)(\eta^2\text{-OAc})]^-$, these interactions occur through carbonyl oxygen atoms of the urea, which are relatively symmetric. For $[M^{II}(H_21)(\eta^1\text{-OAc})]^-$, the potassium ions interact with both the carbonyl and the uncoordinated acetate oxygen atoms. This "bidentate chelation" causes one urea arm to twist away from the M–O$_{\text{acetate}}$ vector, which leads to unsymmetrical H-bonding.

The spectroscopic and structural data for the M^{II}–OAc complexes support the presence of intramolecular H-bonds, yet they appear to be weaker than the corresponding interactions in M^{II}–OH complexes of $[H_33]^{3-}$. In these metal hydroxo complexes, the relevant N $\cdots$ O bond lengths are shorter and $\tilde{\nu}$(NH) signals are lower in energy compared to those found for $[M^{II}(H_21)(\eta^1\text{-OAc})]^-$ and $[M^{II}(H_22)(\eta^2\text{-OAc})]^-$. The average N $\cdots$ O distance in $[Fe^{II}H_33(OH)]^{2-}$ is 2.845 Å and the $\tilde{\nu}$(NH) are 3223 and 3151 cm^{-1},[8c,d] while for $[Co^{II}H_33(OH)]^{2-}$ these values are 2.800 Å and 3227 and 3138 cm^{-1}.[8a,d] These observations most likely reflect delocalization of negative charge within the acetate ligand. This would result in a lowering of the negative charge on the coordinated oxygen atom, which is

also involved in H-bonds. Because H-bonds are predominantly electrostatic interactions, delocalization of charge would weaken the H-bond interactions in the M^{II}–OAc complexes and result in a lengthening of $N \cdots O$ bond distances and an increase in NH vibrations.

Acknowledgements

References and notes

1 (*a*) M. A. Holmes and R. E. Stenkamp, *J. Mol. Biol.*, 1991, **220**, 723; (*b*) V. Fülöp, R. P. Phizackerley, S. M. Soltis, I. J. Clifton, S. Wakatuski, J. Erman, J. Hajdu and S. L. Edwards, *Structure*, 1994, **2**, 201; (*c*) I. Schlichting, J. Berendzen, K. Chu, A. M. Stock, S. A. Maves, D. E. Benson, R. M. Sweet, D. Ringe, G. A. Pestko and S. G. Sligar, *Science*, 2000, **287**, 1615.

2 M. Mukai, S. Nagano, M. Tanaka, K. Ishimori, I. Morishima, T. Ogura, Y. Watanabe and T. Kitagawa, *J. Am. Chem. Soc.*, 1997, **119**, 1758 and references therein.

3 (*a*) B. D. Dunietz, M. D. Beachy, Y. Cao, D. A. Whittington, S. J. Lippard and R. A. Friesner, *J. Am. Chem. Soc.*, 2000, **122**, 2828; (*b*) B. F. Gherman, B. D. Dunietz, D. A. Whittington, S. J. Lippard and R. A. Friesner, *J. Am. Chem. Soc.*, 2001, **123**, 3836.

4 D. R. Tomchick, P. Phan, M. Cymborowski, W. Minor and T. R. Holman, *Biochemistry*, 2001, **40**, 7509.

5 (*a*) C. K. Vance and A.-F. Miller, *Biochemistry*, 2001, **40**, 13079; (*b*) R. A. Edward, M. M. Whittaker, J. M. Whittaker, E. N. Baker and G. B. Jameson, *Biochemistry*, 2001, **40**, 15; (*c*) E. Yikilmaz, J. Xie, T. C. Brunold and A.-F. Miller, *J. Am. Chem. Soc.*, 2002, **124**, 3482; (*d*) J. Xie, E. Yikilmaz, A.-F. Miller and T. C. Brunold, *J. Am. Chem. Soc.*, 2002, **124**, 3769; (*e*) M. S. Lah, M. M. Dixon, K. A. Pattridge, W. C. Stallings, J. A. Fee and M. L. Ludwig, *Biochemistry*, 1995, **34**, 1646.

6 (*a*) G. E. Wuenshell, C. Tetreau, D. Lavalette and C. A. Reed, *J. Am. Chem. Soc.*, 1992, **114**, 3346; (*b*) J. P. Collman, X. Zhang, K. Wong and J. I. Brauman, *J. Am. Chem. Soc.*, 1994, **116**, 6245; (*c*) M. Momenteau and C. A. Reed, *Chem. Rev.*, 1994, **94**, 659; (*d*) J. E. Kickham, S. J. Loeb and S. L. Murphy, *J. Am. Chem. Soc.*, 1993, **115**, 7031; (*e*) D. M. Rudkevich, W. Verboom, Z. Brzozka, M. J. Palys, W. P.R.V. Staut-hamer, G. J. Van Hummel, S. M. Franken, S. Harkema, J. F.J. Engbersen and D. N. Reinhoudt, *J. Am. Chem. Soc.*, 1994, **116**, 4341; (*f*) N. Kitajima, H. Komatsuzaki, S. Hikichi, M. Osawa and Y. Moro-oka, *J. Am. Chem. Soc.*, 1994, **116**, 11596; (*g*) P. H. Walton and K. N. Raymond, *Inorg. Chim. Acta*, 1995, **240**, 593; (*h*) W. Yao and R. H. Crabtree, *Inorg. Chem.*, 1996, **35**, 3007; (*i*) A. Wada, M. Harata, K. Hasegawa, K. Jitsukawa, H. Masuda, M. Mukai, T. Kitagawa and H. Einaga, *Angew. Chem., Int. Ed.*, 1998, **37**, 798; (*j*) C.-Y. Yeh, C. J. Chang and D. G. Nocera, *J. Am. Chem. Soc.*, 2001, **123**, 1513; (*k*) M. Harata, K. Jitsukawa, H. Masuda and H. Einaga, *Chem. Lett.*, 1995, 61; (*l*) A. Wada, M. Harata, K. Hasegawa, K. Jitsukawa, H. Masuda, M. Mukai, T. Kitagawa and H. Einaga, *Angew. Chem., Int. Ed.*, 1998, **37**, 798; (*m*) L. M. Berreau, R. A. Allred, M. M. Makowski-Grzyska and A. M. Arif, *Chem. Commun.*, 2000, 1423; (*n*) L. M. Berreau, M. M. Makowska-Grzyska and A. M. Arif, *Inorg. Chem.*, 2001, **40**, 2212; (*o*) C. Kinblin, X. Bu and A. Bulter, *Inorg. Chem.*, 2002, **41**, 158; (*p*) L. M. Berreau, J. A. Halfen, V. G. Young, Jr. and W. B. Tolman, *Inorg. Chem.*, 1998, **37**, 1091; (*q*) S. Ogo, S. Wada, Y. Watanabe, M. Iwase, A. Wada, M. Harata, K. Jitsukawa, H. Masuda and H. Einage, *Angew. Chem., Int. Ed.*, 1998, **37**, 2102.

7 D. Lee and S. J. Lippard, *J. Am. Chem. Soc.*, 2001, **123**, 4611.

8 (*a*) B. S. Hammes, V. G. Young, Jr. and A. S. Borovik, *Angew. Chem., Int. Ed.*, 1999, **38**, 666; (*b*) Z. Shirin, B. S. Hammes, V. G. Young, Jr. and A. S. Borovik, *J. Am. Chem. Soc.*, 2000, **122**, 1836; (*c*) C. E. MacBeth, A. P. Golombek, V. G. Young, Jr., C. Yang, K. Kuczera, M. P. Hendrich and A. S. Borovik, *Science*, 2000, **289**, 938; (*d*) C. E. MacBeth, B. S. Hammes, V. G. Young, Jr. and A. S. Borovik, *Inorg. Chem.*, 2001, **40**, 4733; (*e*) R. Gupta, C. E. MacBeth, V. G. Young, Jr. and A. S. Borovik, *J. Am. Chem. Soc.*, 2002, **124**, 1136; (*f*) C. E. MacBeth, P. L. Larsen, T. N. Sorrell, D. R. Powell and A. S. Borovik, *Inorg. Chim. Acta*, 2002, **341**, 77; (*g*) P. L. Larsen, T. J. Parolin, D. R. Powell, M. P. Hendrich and A. S. Borovik, *Angew. Chem, Int. Ed.*, 2003, **42**, 85.

9 C. Y. Ng, R. J. Motekaitis and A. E. Martell, *Inorg. Chem.*, 1979, **11**, 2982.

10 A. W. Addison, T. N Rao, J. Reedijk, J. van Rijn and G. C. Verschoor, *J. Chem. Soc., Dalton Trans.*, 1984, 1349.

11 We base this statement on an error of 3σ.

12 The Cambridge Structural Database, www.ccdc.cam.ac.uk, 2002.

13 Selected examples: (*a*) R. A. Reynolds III, W. R Dunham and D. C. Coucouvanis, *Inorg. Chem.*, 1998, **37**, 1232; (*b*) B. Singh, J. R. Long, R. R. de Biani, D. Gatteschi and P. Stavropoulos, *J. Am. Chem. Soc.*, 1997, **119**, 7030; (*c*) K. S. Hagen and R. Lachicotte, *J. Am. Chem. Soc.*, 1992, **114**, 8741; (*d*) S. K. Mandal and L. Que, Jr., *Inorg. Chem.*, 1997, **36**, 5424; (*e*) S. K. Mandal, V. G. Young, Jr. and L. Que, Jr., *Inorg. Chem.*, 2000, **39**, 1831.

14 Selected examples: (*a*) E. M. Holt, S. L. Holt and K. J. Watson, *J. Am. Chem. Soc.*, 1970, **92**, 2721; (*b*) W. D. Horrocks, Jr., J. N. Ishley and R. R. Whittle, *Inorg. Chem.*, 1982, **21**, 3265; (*c*) W. Clegg and B. P. Straughan, *Acta Crystallogr., Sect. B*, 1989, **45**, 1992; (*d*) J.-F. Ma, J.-F. Liu, Y.-C. Liu, Y. Xing, H.-Q. Jia and Y.-H. Lin, *New J. Chem.*, 2000, **24**, 759.

15 E. Bouwman, B. Douziech, L. Gutierrez-Soto, M. Beretta, W. L. Driessen, J. Reedijk and G. Mendoza-Diaz, *Inorg. Chim. Acta*, 2000, **304**, 250.